American Mineralogist, Volume 66, pages 106–117, 1981

The structural role of phosphorus in silicate melts

BJØRN O. MYSEN

Geophysical Laboratory, Carnegie Institution of Washington
Washington, D.C. 20008

FREDERICK J. RYERSON

Department of Terrestrial Magnetism, Carnegie Institution of Washington
Washington, D.C. 20015

AND DAVID VIRGO

Geophysical Laboratory, Carnegie Institution of Washington
Washington, D.C. 20008

Abstract

The influence of P_2O_5 on silicate melt structure has been determined by Raman spectroscopy. The following compositions were studied: NS (Na_2SiO_3), Di ($CaMgSi_2O_6$), Ab ($NaAlSi_3O_8$), An ($CaAl_2Si_2O_8$), Qz (SiO_2), and $NaAl_2PSiO_8$.

In all melts studied P^{5+} is in tetrahedral coordination. Addition of P_2O_5 to melts having a ratio of nonbridging oxygen to the tetrahedral cation (NBO/T) greater than O results in a bulk decrease in this ratio. Phosphate complexes are formed in the melts. These complexes are bonded to metal cations such as Ca^{2+}, Mg^{2+}, and Na^+. The M–PO_4 complexes occur as discrete units that are larger than 20Å in the melt. As a result of the transfer of metal cations from nonbridging oxygens in the silicate portion of the melt structure to the phosphate portion, the NBO/T of the silicate portion is decreased.

Phosphorus is dissolved in quenched SiO_2 melt as discrete sheets of P_2O_5 composition. In three-dimensional aluminosilicate melts (Ab and An), three-dimensional $(AlPO_4)^0$ complexes are formed together with sheet-like P_2O_5 complexes with doubly-bonded oxygen (P = O). As a result of the formation of the $AlPO_4)^0$ complexes, an equivalent amount of Na^+ or Ca^{2+} is no longer needed for local charge balance of Al^{3+}. This metal cation has produced nonbridging oxygen in the melt.

Introduction

Phosphorus is a minor element in most rock-forming silicate melts (generally less than 1 wt. percent P_2O_5). Despite its low abundance, this element has attracted considerable attention because of its strong influence on phase relations and other physical and chemical properties of the melts (*e.g.*, Levin *et al.*, 1969; Kushiro, 1973, 1974, 1975; Watson, 1976; Hess, 1977; Ryerson and Hess, 1978, 1980). Kushiro (1975) noted, for example, that liquidus boundaries between minerals with different degrees of polymerization (*e.g.*, forsterite and protoenstatite) shift rapidly toward the silica-deficient portion of the systems with the addition of P_2O_5.

Liquid immiscibility between basic and acidic melts in both simple and complex systems expands as a result of the addition of P_2O_5 (Watson, 1976; Ryerson and Hess, 1978; Freestone, 1978; Visser and Koster van Groos, 1978). It has been suggested, therefore, that enrichment of phosphorus in late-stage magmas may result in liquid immiscibility (*e.g.*, Rutherford *et al.*, 1974).

Crystal–liquid trace-element partition coefficients depend on melt composition and therefore on the structure of the silicate melt (Watson, 1976, 1977; Hart and Davis, 1978; Irving, 1974). Ryerson and Hess (1978) found that small amounts of P_2O_5 (~1 wt. percent) could alter the values of the trace-element partition coefficients by several hundred per-

0003–004X/81/0102–0106$02.00

cent. They concluded that P_2O_5 critically affects liquid structural features that influence the behavior of crystal–liquid trace-element partitioning.

In view of the petrological importance of the observations summarized above, we decided to conduct a Raman spectroscopic study on selected P-bearing silicate melts. Our aim was to determine the structures of the phosphorus complexes in the melts and to assess the relation between such complexes and the structure of the silicate melt solvent.

Experimental technique

Two groups of compositions were studied. First, phosphorus was added to melts that have a three-dimensional network structure. Second, melts with a significant number of nonbridging oxygens per tetrahedral cation (NBO/T) were considered.

The system SiO_2-P_2O_5 was studied to determine the effect of P_2O_5 on a simple three-dimensional network structure. Other spectroscopic data are also available for this system (*e.g.*, Wong, 1976; Galeener and Mikkelsen, 1979). These results provided reference points for the structural studies of more complex systems. Phophorus was then added to melts of $NaAlSi_2O_8$ (Ab) and $CaAl_2Si_2O_8$ (An) composition. These compositions were chosen partly because feldspars represent a large portion of igneous rocks and partly because of the possibility of Al + P = 2Si substitution in the melt. Such substitution may affect the melt structure. Phosphorus was also added to metasilicate melts of Na_2SiO_3 (NS) and $CaMgSi_2O_6$ (Di) composition. These compositions were selected because metasilicates are important constituents of basaltic rocks. Furthermore, the anionic structure of these depolymerized melts is well known (Brawer and White, 1975; Furukawa and White, 1980; Mysen *et al.*, 1979, 1980; Seifert *et al.*, 1979; Virgo *et al.*, 1980). The relations between the extent of polymerization and the addition of P_2O_5 could thus be studied.

The starting materials were spectroscopically-pure SiO_2, Al_2O_3, MgO, and $CaCO_3$, and reagent-grade Na_2CO_3. Phosphorus was added as a spectroscopically-pure HPO_3 solution. These oxides were thoroughly mixed, melted, and quenched in a platinum-wound vertical quench furnace. The materials were quenched in liquid N_2 at about 500°/sec over the first 1000°C.

The Raman spectra were taken on small bubble-free chips of quenched melts (~0.5–1.0 mm cubes), and were recorded with a Jobin-Yvon optical system, holographic grating, double monochromator (HG25), and a photon-counting detection system, at about 3 cm^{-1}/sec. The iron-free samples were excited with the 488.0 nm line of an Ar^+ laser using a laser power of 200–400 mW at the sample with a 90° scattering geometry. Polarized spectra were obtained with the focused exciting beam parallel to the horizontal spectrometer slit and with the electric vector of the exciting radiation in a vertical orientation. A sheet of polarizer disk in front of an optical scrambler was used to record separately the parallel and perpendicular components of the scattered radiation.

Replicate spectra from the same chips, from different chips of the same experimental run product and from replicate experimental run products were also routinely taken.

Only the frequency region above approximately 700 cm^{-1} shows important spectroscopic features relevant to the structural role of phosphorus, such as the high-frequency stretch vibrations for specific anionic units in the melts (Furukawa and White, 1980; Brawer and White, 1975, 1977; Furukawa *et al.*, 1978; Virgo *et al.*, 1980; Mysen *et al.*, 1980; Bartholemew, 1972; Wong, 1976; Galeener and Mikkelsen, 1979). Only this portion of the spectra is shown in the figures, therefore. The spectral range between 100 and 1400 cm^{-1} was, however, recorded. Because no spectroscopic features are expected above 1400 cm^{-1} (*e.g.*, Galeener and Mikkelsen, 1979), the spectra were not extended further.

The curve-fitting procedure is as follows. In many spectra, individual bands within the high-frequency envelope are not resolved. In these instances, deconvolution of the spectral data is based on spectral information from other systems. Additional support for this procedure stems from the fact that whenever possible the phosphorus contents of a given melt were increased so that new bands or band shifts could be observed as systematic functions of bulk composition.

In metasilicate melts, it is known that Si–O stretch bands indicative of structural units with NBO/Si = 1, 2, and 4 occur near 1070, 970, and 870 cm^{-1}, respectively (Furukawa and White, 1980; see also Mysen *et al.*, 1980, for summary of available data). The presence of these bands in metasilicate melts containing small amounts of P_2O_5 can also be anticipated. Furthermore, we considered it possible that addition of phosphorus may result in structural units similar to those in P-free metasilicate melts, but in which Si has been replaced by P. On the basis of data from other chemical systems, the substitution of Si by P will most likely be reflected in the Raman

spectra by distinct P–O (nonbridging) stretch vibrations characteristic of such anionic units in the melt (Bartholomew, 1972; Nelson and Exharos, 1979) or by (Si,P)–O (nonbridging) stretch vibrations where the individual bands due to Si and P are not differentiated. The above guidelines form the philosophical basis for deconvolution of the metasilicate spectra (*e.g.,* Fig. 1). The positions of the bands are initially adjusted to correspond to the major peak positions of the cumulative envelope. The line profiles are adjusted to Gaussian line shape. Further justification of the proposed spectral model follows, provided that the cumulative area beneath the fitted bands equals that of the high-frequency envelope within statistical uncertainty.

In melts with a three-dimensional network structure, except for the spectra of SiO_2 melt containing 5 mole percent P_2O_5, the high-frequency envelope of the Raman spectra is poorly resolved. The procedure for the curve-fitting is, however, similar to that of phosphorus-bearing metasilicate melts. The frequencies of stretch vibrations due to P–O–P and P–O–Si are known (*e.g.*, Wong, 1976; Galeener and Mikkelsen, 1979), as are those of Si(Al)–O^0 antisymmetric stretching (Virgo *et al.*, 1979; Mysen *et al.*, 1980). This information, the constraints of Gaussian lineshapes, and other information from the raw spectra are used to fit bands in the high-frequency envelope.

Results

In order to provide a framework for band assignments in the melts under consideration, the Raman spectra of quenched melts on various metal oxide–silica joins as a function of metal oxide/silica and type of metal oxide must be considered. A considerable amount of such data is already available (Brawer and White, 1975, 1977; Furukawa *et al.*, 1978; Verweij, 1979a,b; Virgo *et al.*, 1980; Mysen *et al.*, 1980; Virgo and Mysen, in prep.,). This data base includes NBO/Si (nonbridging oxygen per silicon) from near 4 (orthosilicate) to 0 (three-dimensional network) and cations such as K^+, Na^+, Li^+, Ca^{2+}, Mg^{2+}, and Pb^{2+}. In summarizing these data, Brawer and White (1977) and Virgo *et al.* (1980) concluded that the Raman spectra of melts with given metal oxide/silica ratios do not depend on the type of metal cation. It has been inferred from this conclusion that the anionic structure of binary metal oxide–silicate melts does not depend on the type of metal cation (Brawer and White, 1977; Virgo *et al.*, 1980). On the basis of those data, Virgo *et al.* (1980) and Mysen *et al.* (1980) concluded that the structure of silicate melts ranging in bulk composition from orthosilicate to nearly fully polymerized (NBO/T = 0) may be described with the following equations:

for bulk $4 > \text{NBO/T} > 2.1$:

$$T_2O_7^{6-} \rightleftarrows TO_4^{4-} + TO_3^{2-} \quad (1)$$

for bulk $2.1 > \text{NBO/T} > 1.0$:

$$3TO_3^{2-} \rightleftarrows TO_4^{4-} + T_2O_5^{2-} \quad (2)$$

and for bulk $1.0 > \text{NBO/T} > 0.05$:

$$T_2O_5^{2-} \rightleftarrows TO_3^{2-} + TO_2 \quad (3)$$

In equations 1–3, T denotes any tetrahedrally-coordinated cation in the silicate melts.

Metasilicates

The high-frequency envelope of all quenched metasilicate metals (without phosphorus) consists of three symmetric and one antisymmetric stretch band. The three symmetric stretch bands (at ~850, ~950, and 1070–1100 cm^{-1}) correspond to structural units in the melt with, on the average, NBO/Si = 4, 2, and 1 (Verweij, 1979a,b; Furukawa and White, 1980; Virgo *et al.*, 1980; Mysen *et al.*, 1980). In addition, there is an antisymmetric stretch band near 1050 cm^{-1} in all the spectra, a band which most likely stems from antisymmetric stretching of bridging oxygen bonds in the melt (Furukawa and White, 1980). The intensity and frequency of this band is insensitive to variations in bulk composition within the range defined by equation 2 above. For simplicity, this band has not been included in the deconvolution of the spectra.

Up to 2 mole percent P_2O_5 (O = 6) was added to melts of Di and NS composition (Table 1). The resulting Raman spectra of quenched NS melt are shown in Figure 1. Addition of P_2O_5 results in two new bands near 900 and 1000 cm^{-1}. In addition, the frequency of the two stretch bands reflecting polymerized silicate units in the melts (chains and sheets) is lowered slightly, and their intensity ratios are altered (Fig. 2). In phosphorus-free, quenched NS melt, the 970 cm^{-1} band (diagnostic of $Si_2O_6^{4-}$ chains) is predominant (Fig. 1). This band diminishes in intensity relative to the 1070 cm^{-1} band ($Si_2O_5^{2-}$ sheets) as the P_2O_5 content of the quenched melt is increased (Fig. 2). Monomers and chains ($Si–O^{2-}$ stretch, 850 cm^{-1}; $^-O–Si–O^-$ stretch, 970 cm^{-1}) persist with up to 2 mole percent P_2O_5 in solution in quenched Di melt. The intensity of the 970 cm^{-1} band decreases faster than that of the 880 cm^{-1} band (Fig. 2).

Table 1. Raman data of depolymerized melts with P_2O_5

Composition	Temperature, °C	Wavenumber, cm^{-1}*						
$CaMgSi_2O_6$	1575	632s	...	880m	...	980s	...	1070m
$CaMgSi_2O_6$ + 1 mole % P_2O_5	1575	630s	...	875m	915w	947s	1000w	1047s
$CaMgSi_2O_6$ + 2 mole % P_2O_5	1575	633s	660(sh)	875m	900w	950s	987m	1043s
Na_2SiO_3	1400	620s	...	847mw	...	979s	...	1065m
Na_2SiO_3 + 2 mole % P_2O_5	1400	600s	660(sh)	843w	920s	950s	982s	1041s

*Abbreviations: s, strong; ms, medium to strong; m, medium; mw, medium to weak; w, weak; vw, very weak; (bd), broad; (sh), shoulder.

The bands that appear near 1000 and 900 cm^{-1} with P_2O_5 in quenched NS melt reflect P–O stretch vibrations (Bartholomew, 1972; Wong, 1976; Nelson and Exharos, 1979). These bands probably reflect vibrations in P–O tetrahedra that contain nonbridging oxygens because (1) there is no P=O (doubly-bonded oxygen) stretch band present and (2) their intensities are considerably greater than those of $P–O^0$ vibrations in quenched SiO_2–P_2O_5 and P_2O_5 melts (Galeener and Mikkelsen, 1979; Wong, 1976). Furthermore, the frequencies of possible P–O–Si and P–O–P vibrations found in the system SiO_2–P_2O_5 are at 1100 and 970 cm^{-1}, respectively (Wong, 1976), and thus differ from the positions observed here. Bartholomew (1972) studied the vibrational spectra of quenched melts in the system Ag_2O–P_2O_5. On the basis of his results and the above arguments, we conclude that the band at 1000 cm^{-1} results from $^0O–P–O^-$ stretching, and the band at 900 cm^{-1} from $^-O–P–O^-$ stretch vibration in the system Na_2SiO_3–P_2O_5. That is, phosphorus may exist in sheets or chains. The presence of separate bands derived from vibrations in these structural units rather than coupling of the Si–O stretch bands indicates that discrete phosphate complexes exist together with silicate monomers, chains, and sheets in the quenched melts of NS composition with 2 mole percent P_2O_5.

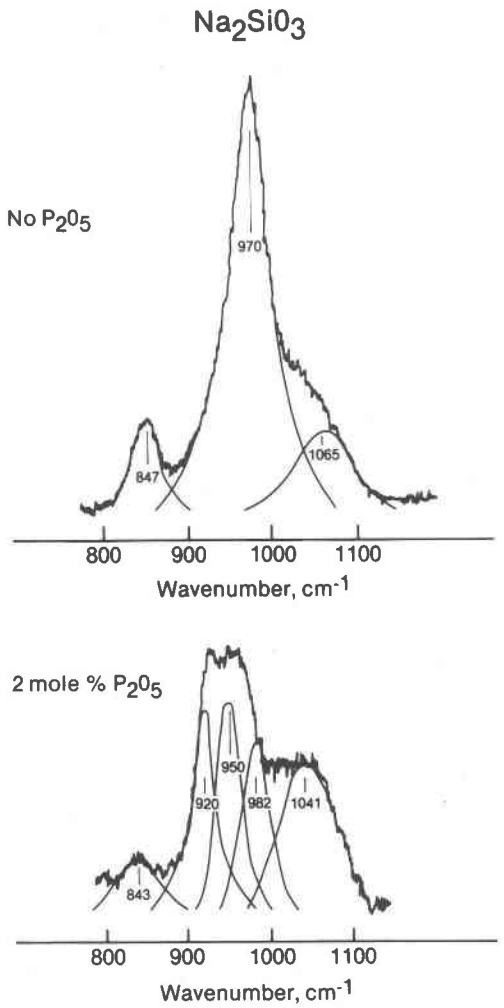

Fig. 1. Unpolarized Raman spectra of quenched melt of Na_2SiO_3 composition as a function of P_2O_5 content.

Inasmuch as the intensity ratios, $I(1070)/I(980)$, $I(1070)/I(880)$, and $I(1000)/I(900)$, increase with increasing phosphorus content (Fig. 2), we conclude that sheet units of both silicate and phosphate are the favored structural units in P_2O_5-bearing, quenched Di melt. Teus the solution of P_2O_5 in such melts results in an increased degree of polymerization (NBO/T has decreased).

The Raman spectroscopic data on quenched melt of $CaMgSi_2O_6$ composition with P_2O_5 indicate that this melt and that of Di composition respond similarly to dissolved P_2O_5 (Figs. 1 and 3; see also Table 1). The two new bands near 920 and 1000 cm^{-1} are due to P–O vibrations, and the frequencies of the 1070 and 970 cm^{-1} bands shift as they do for NS + P_2O_5. Furthermore, sheet units become more domi-

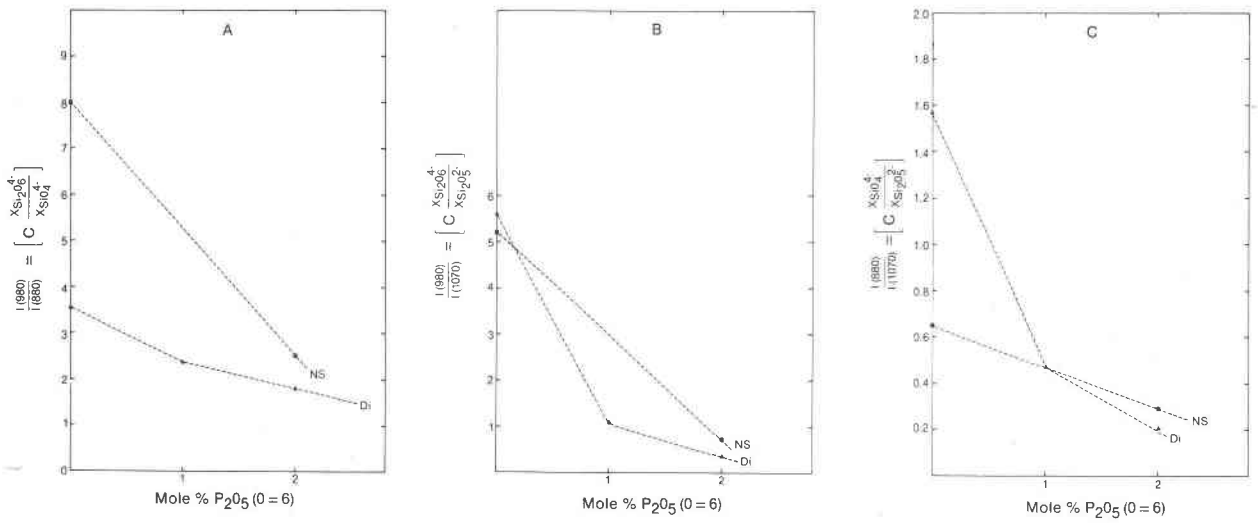

Fig. 2. Intensity ratios of Raman bands diagnostic of monomers, chains, and sheets in metasilicate melts as a function of P_2O_5 content. (A) $I(980)/I(880)$ (proportion of chain to monomer). (B) $I(980)/I(1070)$ (proportion of chain to sheet). (C) $I(880)/I(1070)$ (proportion of monomer to sheet).

nant with increasing P_2O_5 content of the melt [$I(1070)/I(950)$ and $I(1070)/I(850)$ increase]. In fact, the $^-$O–Si–O^0 symmetric stretch band is the main band in the high-frequency envelope with 2 mole percent P_2O_5 in solution in quenched Di melt (Fig. 3).

In summary, solution of P_2O_5 in metasilicate melts has two results. First, silicate sheet units become more dominant relative to less polymerized structural units such as chains and monomers. Second, decoupled (discrete) phosphate units with nonbridging oxygens may be formed.

Melts with a three-dimensional network structure

The system SiO_2–P_2O_5 is used as a reference system for band assignments in the more complex aluminosilicate melts with a three-dimensional network structure.

Addition of 5 mole percent P_2O_5 to SiO_2 results in the appearance of three new stretch bands reflecting P–O and P=O stretch vibrations in the frequency range between 900 and 1400 cm^{-1} (Fig. 4; see also Table 2). The two original stretch vibrations with bands near 1065 and 1200 cm^{-1} (Bates *et al.*, 1974) remain. The sharp band at 1322 cm^{-1} is due to P=O^0 stretching (*e.g.*, Wong, 1976; Galeener and Mikkelsen, 1979). The position of this band agrees with that observed by Wong for quenched melts of similar compositions. The band near 1100 cm^{-1} corresponds to P–O–Si stretching (P–O^0), and that near 1000 cm^{-1}, to P–O–P stretching (Wong, 1976). No nonbridging oxygens result from solution of P_2O_5 in SiO_2 melt. The structure contains defects, however, as a result of termination of the network at the double-bonded oxygens (P=O).

The high-frequency envelope of the Raman spectrum of quenched $NaAl_2PSiO_8$ melt consists of four bands (Fig. 5). There is a broad band near 1170 cm^{-1}. Inasmuch as there is no P–O vibration at or near this frequency, the 1170 cm^{-1} band is assigned to an (Si,Al)–O^0 stretch vibration. The large frequency increase of this band relative to its position in phosphorus-free, quenched Ab melt (~1090 cm^{-1}; see Mysen *et al.*, 1980) probably results from a substantial increase of Si/(Si + Al) of the three-dimensional structural units from which this band is derived (Virgo *et al.*, 1979). The 1056 cm^{-1} band (Fig. 5) probably corresponds to the 991 cm^{-1} band in phosphorus-free, quenched Ab melt [see Virgo *et al.* (1979) and Mysen *et al.* (1980) for discussion of the structure of $NaAlSi_3O_8$ melt] and the 1065 cm^{-1} band in quenched SiO_2 melt [see Fig. 4 and also Bates *et al.* (1974) for discussion of the structure and Raman spectra of SiO_2 melt]. The frequency increase of the lowest-frequency (Si,Al)–O^0 antisymmetric stretch band is a direct consequence of the increased Si/(Si + Al) of the aluminum silicate portion of the melt, as already indicated by the increase of the 1090 cm^{-1} band to 1170 cm^{-1} [see also Virgo *et al.* (1979) for discussion of the response of the two antisymmetric (Si,Al)–O^0 stretch bands of melts on the join $NaAlSiO_4$–SiO_2 as a function of bulk composition].

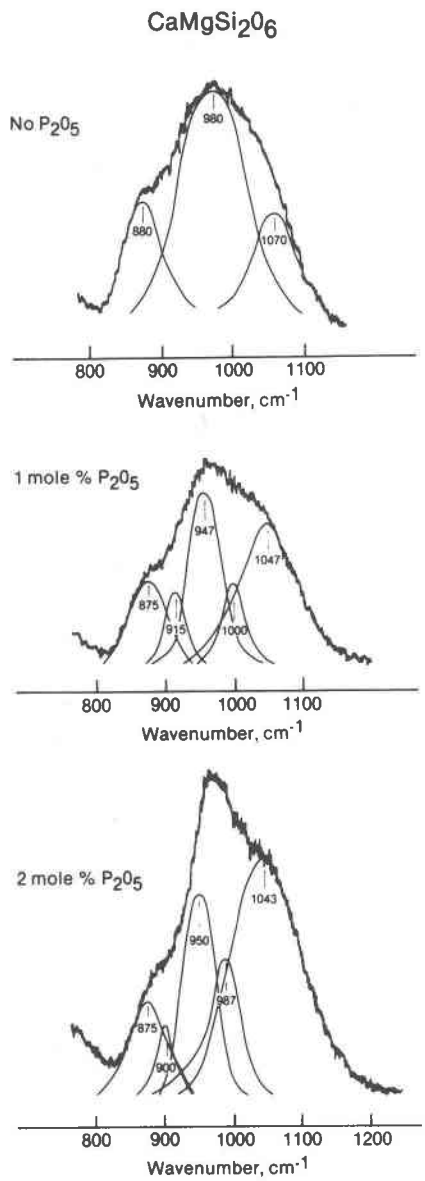

Fig. 3. Unpolarized Raman spectra of quenched Di melt as a function of P_2O_5 content.

From the calibration curve of Virgo *et al.* (1979) reproduced in Figure 6, it can be calculated that the Si/(Si + Al) of the two three-dimensional units is near 0.95 in quenched $NaAl_2PSiO_8$ melt, although the bulk Si/(Si + Al) of this composition is 0.33. The existence of nearly pure SiO_2 three-dimensional network units in quenched $NaAl_2PSiO_8$ melt is further substantiated by the occurrence of two Si–O^0 rocking bands at 424 and 467 cm^{-1} (Fig. 5). These two bands occur at the same frequency (within experimental uncertainty) in quenched SiO_2 melt (Bates *et al.*, 1974). With any significant amount of Al in the three-dimensional network units, only one (Si,Al)–O^0 rocking band can be found. This band occurs between 470 and 500 cm^{-1}, depending on Si/(Si + Al) (Virgo *et al.*, 1979).

The 1073 cm^{-1} band in the high-frequency envelope of quenched $NaAl_2PSiO_8$ melt probably corresponds to the 1100 cm^{-1} band in the spectrum from quenched SiO_2–P_2O_5 melt (Galeener and Mikkelsen, 1979), in which the 1100 cm^{-1} band was assigned to Si–O–P stretching. The frequency of this band in the spectrum from quenched $NaAl_2PSiO_8$ melt may be lower because the band stems from Al–O–P rather than Si–O–P stretching. A close structural association of Al^{3+} and P^{5+} may also help to explain the diminished role of Al^{3+} in the three-dimensional (Al,Si) structural units in the melt.

The apparent existence of a three-dimensional

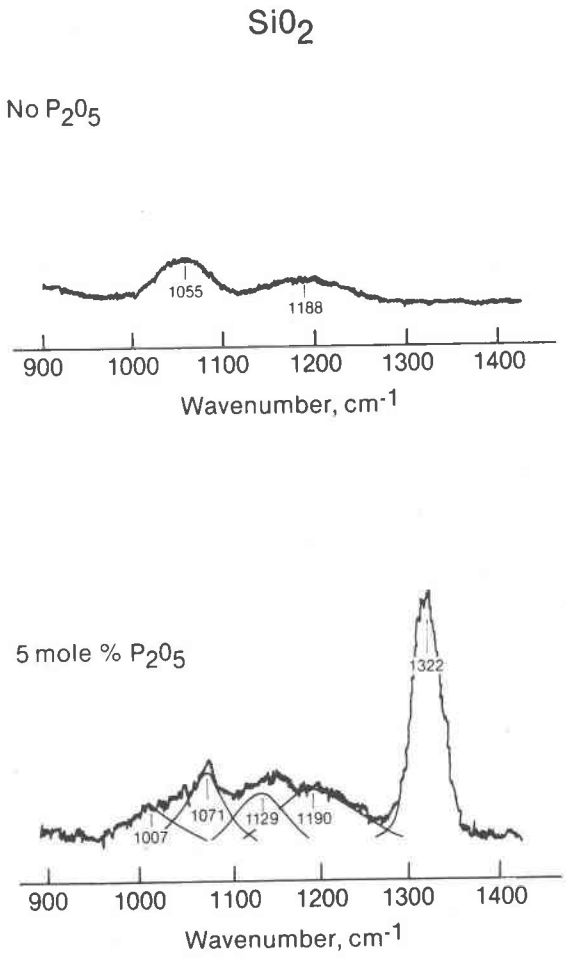

Fig. 4. Unpolarized Raman spectra of quenched melts on the join SiO_2–P_2O_5.

Table 2. Raman data of quenched melts in the system $CaO–Na_2O–Al_2O_3–SiO_2–P_2O_5$

Composition	T°C	Wavenumber, cm^{-1}									
SiO_2	1800	430s	484s	595w	790m	...	...	1055w	...	1180w	...
SiO_2 + 5 mole % P_2O_5	1650	414s	474(sh)	601w	781m	...	1007w	1071m	1129m	1190m	1322s
$CaAl_2Si_2O_8$	1575	...	500s	575(sh)	750(sh)	...	...	950m	...	1000s	...
$CaAl_2Si_2O_8$ + 2 mole % P_2O_5	1575	...	496s	564(sh)	770(sh)	926m	...	986s	1040w	1080s	...
$CaAl_2Si_2O_8$ + 5 mole % P_2O_5	1575	449(sh)	498s	561(sh)	780(sh)	920m	...	982s	1033m	1095s	1284w
$NaAlSi_3O_8$	1575	...	470s	566(sh)	780(sh)	...	...	991s	...	1095s	...
$NaAlSi_3O_8$ + 5 mole % P_2O_5	1575	435(sh)	468s	578w	796w	964w	...	998s	1072m	1130s	1250w
$NaAl_2PSiO_8$	1575	424m(bd)	467s(bd)	590(sh)	755(sh)	971w(bd)	...	1056s	1073s	1173m(bd)	

Abbreviations as in Table 1.

aluminum phosphate unit in $NaAl_2PSiO_8$ melt indicates a possible origin of the 971 cm^{-1} band (Fig. 5). The association of Al^{3+} and P^{5+} results in both Al and P being charge-balanced in tetrahedral coordination without the aid of an alkali. As a result, an amount of Na^+ equivalent to that of Al^{3+} in the aluminum phosphate unit is no longer needed for local charge balance of the aluminum. This Na^+ acts as a network modifier to form nonbridging oxygens in the melt. The 971 cm^{-1} band results from a stretch vibration in a silicate complex with NBO/T > 0. In the absence of an indication of P–O–P bonds [expected near 1100 cm^{-1} according to Galeener and Mikkelsen (1979)] in the aluminum phosphate complex, its Al/P must be about 1. Since the bulk Al/P = 2, and bulk Al/Si = 2 in the $NaAl_2PSiO_8$ composition and Si/(Si + Al) = 0.95 in the aluminum silicate complexes with a three-dimensional network structure, the 971 cm^{-1} band must stem from a vibration in a structural unit with a large Al/Si. The Al-free $^-O–Si–O^-$ stretch vibration results in a band near 950 cm^{-1} (*e.g.*, Brawer and White, 1975). Coupled $^-O–(Al,Si)–O^-$ vibrations result in bands at even lower frequency (Virgo *et al.*, 1979). The 971 cm^{-1} band is probably a strongly coupled (Si,Al)–O vibration from a structural unit with NBO/T < 2. The unit could be a sheet, for example, since $^-O–(Si,Al)–O^0$ stretch bands from quenched melts of $NaCaAlSi_2O_7$ composition occur near 980 cm^{-1} (Mysen and Virgo, 1980).

In summary, the anionic structure of quenched $NaAl_2PSiO_8$ melt consists of two (Si,Al) three-dimensional units with Si/(Si + Al) about 0.95, a decoupled three-dimensional $AlPO_4$ unit, and an (Si,Al) structural unit with 0 < NBO/T < 2, which could be a sheet.

The high-frequency envelope of quenched Ab melt

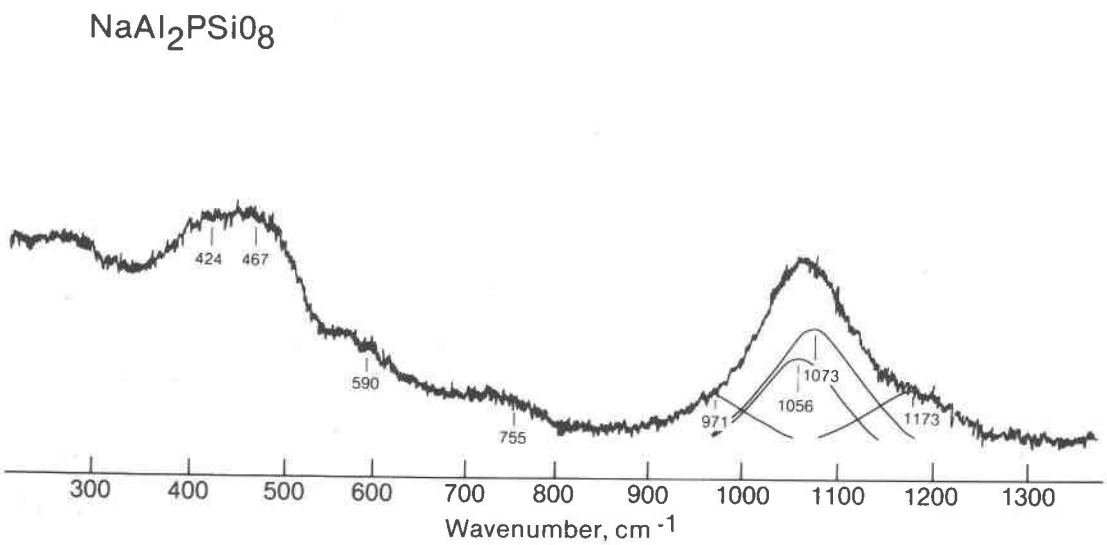

Fig. 5. Unpolarized Raman spectrum of quenched melt of $NaAl_2PSiO_8$ composition.

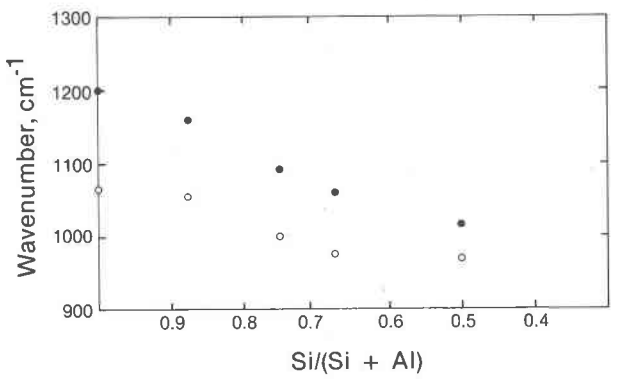

Fig. 6. Frequencies of the two (Si,Al)–O^0 stretch bands in melts with a three-dimensional network structure on the join $NaAlO_2$–SiO_2 as a function of Si/(Si + Al).

with 5 mole percent P_2O_5 resembles that of quenched $NaAl_2PSiO_8$ (Figs. 5 and 7) in that the same bands are found in both. In addition, there is a weak band near 1250 cm^{-1}, which is assigned to P=O stretching. The exact frequency of this band depends strongly on the electric field in the vicinity of the P=O bond (Bartholomew, 1972), which explains the difference in the frequencies of this band in SiO_2–P_2O_5 and $NaAlSi_3O_8$–P_2O_5 quenched melts (Figs. 4 and 7). The band corresponding to the 1100 cm^{-1} band in quenched SiO_2–P_2O_5 melt (Si–O–P stretching) occurs near 1070 cm^{-1} in quenched Ab + 5 mole percent P_2O_5 melt and also in quenched $NaAl_2PSiO_8$ melt (Figs. 4, 5 and 7). It is, therefore, probably the Al–O–P stretch band.

As a result of some Al^{3+} associating with P^{5+}, the remaining aluminosilicate units of the three-dimensional network become less aluminous, as also argued above for quenched $NaAl_2PSiO_8$ melt. Consequently, the (Al,Si)–O^0 stretch bands found at 991 and 1095 cm^{-1} in quenched Ab melt (Fig. 7) would be shifted to higher frequencies (Virgo *et al.*, 1979). The bands are at 998 and 1130 cm^{-1} with 5 mole percent P_2O_5 in solution (Fig. 7). The high-frequency band shifts more than the low-frequency band as a function of increasing Si/(Si + Al) (Virgo *et al.*, 1979). According to their calibration curve of these bands (Fig. 6), a shift of the 990 cm^{-1} band to near 1000 cm^{-1} and of the 1095 cm^{-1} band to near 1130 cm^{-1} corresponds to an increase of Si/(Si + Al) of the two three-dimensional (Si,Al) units of the Ab melt of 5 and 15 percent, respectively. The bulk increase of the Si/(Si + Al) of the aluminosilicate portion of the melt cannot be determined because the proportion of the two network units is not known.

The weak band at 964 cm^{-1} (Fig. 7) most likely corresponds to the 971 cm^{-1} band in quenched $NaAl_2PSiO_8$ melt (Figs. 5 and 7). Therefore this band probably is due to the existence of similar structural units [(Si,Al) unit with $0 < NBO/T < 2$] in both melts.

In summary, it appears that the following structural units can be discerned in quenched Ab melt with 5 mole percent P_2O_5: discrete P_2O_5 units with a sheet structure but without nonbridging oxygen (due to the presence of P=O bonds); two three-dimensional network units of (Si,Al) with Si/(Si + Al) 5–15 percent greater than in phosphorus-free, quenched Ab melt; discrete aluminum phosphate units that occur as a three-dimensional network; finally, there is a proportion of an (Si,Al) unit that contains nonbridging oxygen, with $0 < NBO/T < 2$.

Raman spectra of quenched melt of $CaAl_2Si_2O_8$ composition with up to 5 mole percent P_2O_5 are shown in Figure 8 (see also Table 2). With 2 mole percent P_2O_5, four bands appear in the high-fre-

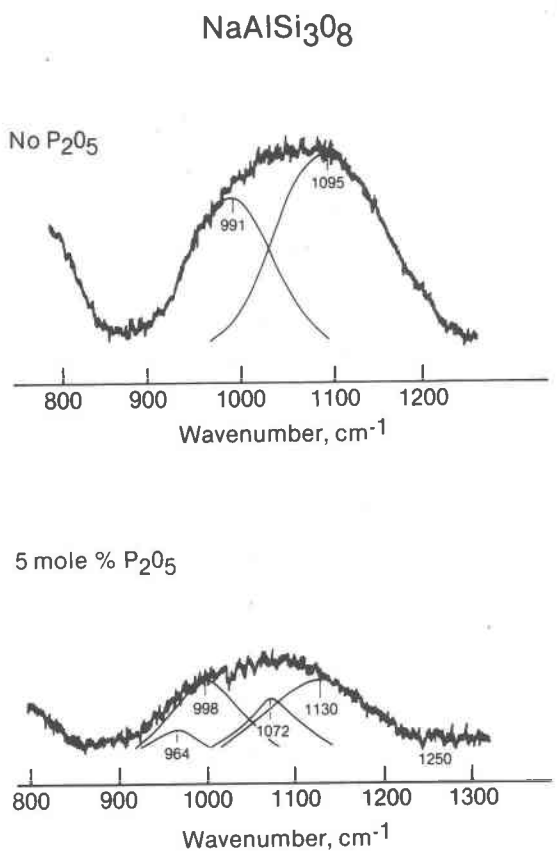

Fig. 7. Unpolarized Raman spectra of quenched melts on the join $NaAlSi_3O_8$–P_2O_5.

quency envelope (926, 986, 1040, and 1080 cm^{-1}). The same four bands occur with 5 mole percent P_2O_5. The 1080 cm^{-1} band has shifted to slightly higher frequency, however, compared with P_2O_5-free An melt.

We suggest that the 1030 cm^{-1} band reflects vibrations involving P–O bonds and corresponds to the 1072 cm^{-1} band in quenched, phosphorus-bearing Ab melt (Table 2). The lower frequency in An melt is probably caused by more extensive (P,Al) coupling, as the An melt is more aluminous than the Ab melt.

In analogy with the arguments to assign the 1000 and 1130 cm^{-1} bands in quenched, phosphorus-bearing Ab melt, the 980 and 1080 cm^{-1} bands in quenched phosphorus-bearing An melt reflect (Si, Al)–O^0 stretching. The frequency shifts as a function of Si/(Si + Al) correspond to about a 25 percent increase in the latter ratio.

The band near 920 cm^{-1} is a stretch band reflecting nonbridging oxygen generated as a result of the formation of aluminum phosphate units in the An melt. The reasoning is the same as that for quenched, phosphorus-bearing Ab melt. Its lower frequency in the former melt is due to lower Si/(Si + Al) of An compared with Ab composition, resulting in a greater Al content in the depolymerized (Si,Al) unit, or it is due to greater NBO/T of the unit in quenched, phosphorus-bearing An melt than in the analogous Ab melt. We cannot determine which interpretation is correct.

With the addition of 5 mole percent P_2O_5, an additional weak band appears near 1284 cm^{-1} (Fig. 8). This band reflects P=O stretching.

In summary, solution of P_2O_5 in An melt results in the same structural units as in phosphorus-bearing Ab melt. These units are one P_2O_5 sheet (with P=O and no NBO), two (Si,Al) three-dimensional units with higher Si/(Si + Al) than in phosphorus-free An melt, a three-dimensional aluminum phosphate unit, and a unit with Si and Al in tetrahedral coordination and with some nonbridging oxygen.

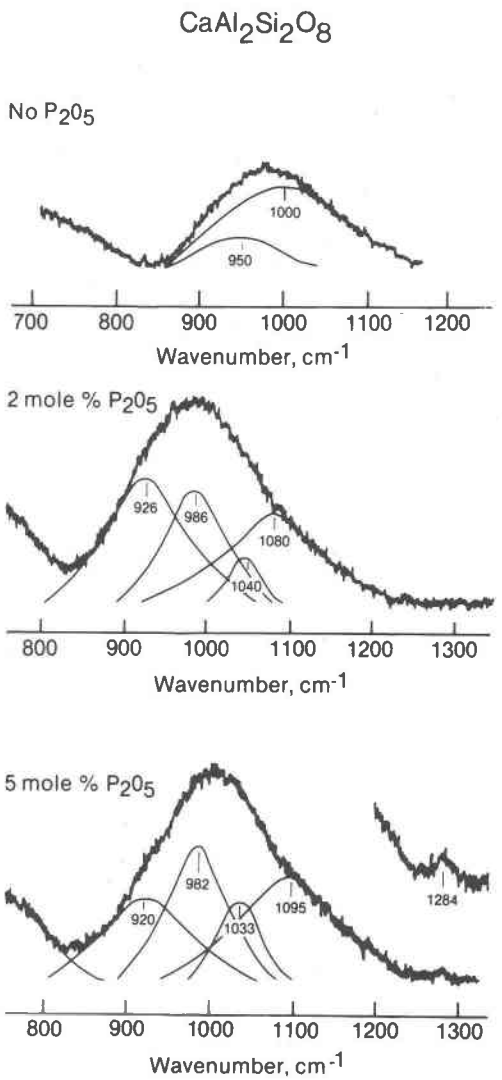

Fig. 8. Unpolarized Raman spectra of quenched melts on the join $CaAl_2Si_2O_8$–P_2O_5.

Melts *vs.* quenched melts

In this study, quenched melts (glass) have been used to determine the structure of molten silicates. In order to relate the structural information from quenched melts to structural features of silicate melts, it is necessary to document that the structural features under consideration are not significantly affected by quenching. Riebling (1968) and Taylor *et al.* (1980) found that the anionic units (silicate polymers) in melts with a three-dimensional network structure, such as melts of $NaAlSi_3O_8$ composition, remain the same when the melt is quenched to a glass. Direct experimental proof of structural similarity between melts and their quenched analogues on the join Na_2O–SiO_2 was provided by Sweet and White (1969) and Sharma *et al.* (1978), who compared infrared and Raman spectra of melts of $Na_2Si_3O_7$, $Na_2Si_2O_5$, and Na_2SiO_3 composition with those of their glasses. They concluded that the structures of these melts and glasses were similar, as there were no discernible differences between the spectra of the two forms of the same compositions.

On the basis of this information, we conclude that the structural features of silicate melts that can be determined with Raman spectroscopy are quenchable.

Our results are therefore believed to be applicable to molten silicates.

Solubility mechanisms

Phosphorus is in tetrahedral coordination in the melt compositions studied here. In melts with NBO/T > 0, PO_4^{3-} tetrahedra appear to prefer sheet structures at the expense of chains and monomers. These sheets are not terminated by P=O bonds, in contrast to the structural features of P_2O_5 glass (Galeener and Mikkelsen, 1979).

Because of the greater stability of P–O–M than of Si–O–M bonds, the former bonds would be favored (Ryerson and Hess, 1980), thus resulting in polymerization of the silicate portion of the melt. Our data indicate that phosphate units in the melts dominate as a sheet structure and that such sheet units do not have the doubly-bonded oxygen found in P_2O_5 glass (Galeener and Mikkelsen, 1979). We suggest, therefore, as did Ryerson and Hess, that the following reaction takes place:

$$\begin{aligned} &\begin{array}{c} | \\ O^0\text{–}P \\ | \end{array} = O^0 + 2M\text{–}O^-\text{–}\begin{array}{c} | \\ Si\text{–} \\ | \end{array} \\ &\qquad \rightleftarrows \begin{array}{c} | \\ O^0\text{–}P\text{–}O^-\text{–}M \\ | \end{array} + \begin{array}{c} | \\ \text{–}Si\text{–}O\text{–}Si\text{–}O^-\text{–}M \\ | \end{array} \end{aligned} \qquad (4)$$

where a nonbridging oxygen (O^-) in the silicate network is lost and a new bridging oxygen (O^0) is formed by the formation of the metal (M) phosphate complex. The proportions of chains and sheets increase relative to that of monomers.

The Raman spectrum of quenched melt in the system SiO_2–P_2O_5 indicates that it consists of a mixture of three-dimensional SiO_2 and P_2O_5 sheets (the latter has no NBO). Inasmuch as the phosphorous unit is terminated by a P=O bond, there is no nonbridging oxygen in the structure. Therefore, despite the pronounced influence of P_2O_5 on the liquidus temperature of SiO_2 (see, *e.g.*, Levin *et al.*, 1969, p. 142), P^{5+} is not a network modifier in melt of SiO_2 composition.

Solution of P_2O_5 in aluminosilicate melts with a three-dimensional network structure appears to result in two different structural changes of the melt. With 5 mole percent P_2O_5, the existence of a Raman band diagnostic of P=O indicates that sheet units with no NBO occur in these melts. These units may resemble those found in melts in the system SiO_2–P_2O_5. The Raman data also indicate that some of the P^{5+} is closely associated with Al^{3+}. Ryerson and Hess (1980) concluded similarly, on the basis of chemical and physical properties of phosphorus-bearing aluminosilicate melts. They suggested that three-dimensional complexes of the type $AlPO_4$ or $NaAl_2PSiO_8$ may occur. The only difference between the two units is that in $NaAl_2PSiO_8$, $NaAlO_2$ (or $CaAl_2O_4$ in the case of $Ca_2Al_5PSi_2O_{16}$), $AlPO_4$, and SiO_2 tetrahedra are randomly mixed, whereas in the case of $AlPO_4$ alone, the presence of discrete domains or structones (in the terminology of Fraser, 1977) may exist. There is no evidence for Si–O–P bonds in the melts, as the latter type of bonds would result in stretch vibrations with a Raman band at 1100 cm^{-1} (Wong, 1976). Inasmuch as such bonds would be encountered in $NaAl_2PSiO_8$ complexes, the existence of this complex in phosphorus-bearing aluminosilicate melts is ruled out. Stretch vibrations from P–O–P bonds would result in a Raman band near 970 cm^{-1} (Wong, 1976) but are not encountered in the spectra of the aluminosilicate melts. Only Al–O–P stretch bands seem to exist. Consequently, an aluminophosphate complex with P/Al about 1 is likely. A phosphate complex of the type $AlPO_4$ is therefore suggested.

Applications

Kushiro (1973, 1974, 1975) found that among all the oxides added to the melts, P_2O_5 had the most pronounced effect on the liquidus boundaries between forsterite and protoenstatite and between pseudowollastonite and cristobalite. The phosphate complexes in depolymerized melts are not randomly distributed in the melt structures but occur as discrete units. Their physical presence does not affect the silicate equilibria. These units are formed by interaction between modifying cations derived from the silicate portion of the system and the doubly-bonded oxygen in the added phosphate (equation 1). A new bridging oxygen is formed in the silicate per each doubly-bonded oxygen in the added phosphate. The doubly-bonded oxygen becomes singly-bonded to form M–O–P. This polymerization mechanism explains the dramatic effect of P_2O_5 on the liquidus boundaries studied by Kushiro.

Watson (1976) and Ryerson and Hess (1980) noted that trace-element partitioning between immiscible acidic and basic melts in equilibrium is strongly influenced by P_2O_5. Rare-earth elements (REE) are partitioned more strongly into the basic melt in the presence of P_2O_5. Since the decrease of NBO/T of the basic melt affected by phosphorus would indicate the opposite effect, we conclude, as did Ryerson and Hess (1980), that REE^{3+} form phosphate complexes in the melt. The REE phosphates in basic melt are more stable than those in the acidic melts.

Ryerson and Hess noted that alkali metals show a stronger preference for the acidic melt than for the immiscible basic melt when P_2O_5 is present. We suggest that this behavior is related to the depolymerizing effect of P_2O_5 in highly polymerized aluminosilicate melts (to form $AlPO_4$ complexes and network-modifying metal cations).

Solution of phosphorus in highly polymerized silicate melts is likely to result in a substantial reduction in the melt viscosity. This reduction is a result of new nonbridging oxygens in such melts. In view of the model for viscous flow of such melts by Mysen *et al.* (1980), it is possible that the melt viscosity will increase with increasing pressure, whereas the viscosity of the phosphorus-free analogues decreases (Kushiro, 1976, 1978). It is difficult to predict the influence of P_2O_5 on the viscosity of melts with a significant proportion of NBO/T (greater than 1). If the only flow units are SiO_4^{4-} monomers, as is the case in the phosphorus-free analogues, it is likely that the viscosity will increase with solution of P_2O_5 as the NBO/T decreases. It is possible, however, that both phosphates and silicates act as flow units. In this case, the strength of P–O–Si and P–O–P bonds may be critical. In view of the charge imbalance of P^{5+} and Si^{4+} in tetrahedral coordination, we suggest that P–O–Si bonds are weaker than Si–O–Si bonds. Under these circumstances, the solution of phosphorus in depolymerized melts will result in a lowering of the melt viscosity.

Acknowledgments

Critical reviews by D. H. Eggler, C. M. Scarfe, I. Kushiro, W. B. White, and H. S. Yoder, Jr. are appreciated. Extensive discussions with Dr. Kushiro during the final stages of this research greatly improved the manuscript. This research was supported partly by NSF grant EAR 7911313 and partly by the Carnegie Institution of Washington.

References

Bartholomew, R. F. (1972) Structure and properties of silver phosphate glasses—infrared and visible spectra. Journal of Non-Crystalline Solids, 7, 221–235.

Bates, J. B., Hendricks, R. W., and Shaffer, L. B. (1974) Neutron irradiation effects and structure of non-crystalline SiO_2. Journal of Chemical Physics, 61, 4163–4176.

Brawer, S. A. and White, W. B. (1975) Raman spectroscopic investigation of the structure of silicate glasses. I. The binary silicate glasses. Journal of Chemical Physics, 63, 2421–2432.

Brawer, S. A. and White, W. B. (1977) Raman spectroscopic investigation of the structure of silicate glasses (II) soda-alkaline earth–alumina ternary and quaternary glasses. Journal of Non-Crystalline Solids, 23, 261–278.

Fraser, D. G. (1977) Thermodynamic properties of silicate melt. In D. G. Fraser, Ed., Thermodynamics in Geology, p. 301–325. Proceedings of NATO Advanced Study Institute, Oxford, England, Sept. 1976.

Freestone, I. C. (1978) Liquid immiscibility in alkali-rich magmas. Chemical Geology, 23, 115–124.

Furukawa, T. and White, W. B. (1980) Raman spectroscopic investigation of the structure of silicate glasses. III. Alkali-silico-germanates. Journal of Chemical Physics, in press.

Furukawa, T., Brawer, S. A., and White, W. B. (1978) The structure of lead silicate glasses determined with vibrational spectroscopy. Journal of Materials Science, 13, 268–282.

Galeener, F. L. and Mikkelsen, J. C. (1979) The Raman spectra and structure of pure vitreous P_2O_5. Solid State Communication, 20, 505–510.

Hart, S. E., and Davis, K. E. (1978). Nickel partitioning between olivine and silicate melt. Earth and Planetary Science Letters, 40, 203–220.

Hess, P. C. (1977) Structure of silicate melts. Canadian Mineralogist, 15, 162–178.

Irving, A. J. (1978) A review of experimental studies of crystal/liquid trace element partitioning. Geochimica et Cosmochimica Acta, 42, 743–771.

Kushiro, I. (1973) Regularities in the shift of liquidus boundaries in silicate systems and their significance in magma genesis. Carnegie Institution of Washington Year Book, 72, 497–502.

Kushiro, I. (1974) Pressure effect on the changes of the forsterite–enstatite liquidus boundary with the addition of other cations and the genesis of magmas. Carnegie Institution of Washington Year Book, 73, 238–251.

Kushiro, I. (1975) On the nature of silicate melt and its significance in magma genesis. Regularities in the shift of liquidus boundaries involving olivine, pyroxene, and silica minerals. American Journal of Science, 275, 411–431.

Kushiro, I. (1976) Changes in viscosity and structure of melt of $NaAlSi_2O_6$ composition at high pressure. Journal of Geophysical Research, 81, 6347–6350.

Kushiro, I. (1978) Viscosity and structural changes of albite ($NaAlSi_3O_8$) melt at high pressures. Earth and Planetary Science Letters, 41, 87–91.

Levin, E. M., Robbins, C. R., and McMurdie, H. F. (1969) Phase diagrams for ceramists. 1969 supplement. American Ceramic Society, Columbus, Ohio.

Mysen, B. O. and Virgo, D. (1980) Solubility mechanisms of CO_2 in silicate melts. American Mineralogist, 65, 885–899.

Mysen, B. O., Virgo, D., and Scarfe, C. M. (1980) Relations between anionic structure and viscosity of silicate melts—a Raman spectroscopic study at 1 atm and at high pressure. American Mineralogist, 65, 690–711.

Mysen, B. O., Virgo, D., and Seifert, F. (1979) Melt structure and redox equilibria in the system $CaO–MgO–FeO–Fe_2O_3–SiO_2$. Carnegie Institution of Washington Year Book, 78, 519–526.

Nelson, B. N. and Exharos, G. J. (1979) Vibrational spectroscopy of cation-site interactions in phosphate glasses. Journal of Chemical Physics, 71, 2739–2747.

Riebling, E. F. (1968) Structural similarities between a glass and its melt. Journal of American Ceramics Society, 51, 143–149.

Rutherford, M. J., Hess, P. C., and Daniel, G. H. (1974) Experimental liquid line of descent and liquid immiscibility for basalt 100017. Proceedings 5th Lunar Science Conference, 1, 569–583.

Ryerson, F. J. and Hess, P. C. (1978) The partitioning of trace elements between immiscible silicate melts. (abstr.) EOS, 56, 470.

Ryerson, F. J. and Hess, P. C. (1980) The role of P_2O_5 in silicate melts. Geochimica et Cosmochimica Acta, 44, 611–625.

Sharma, S. K., Virgo, D. and Mysen, B. O. (1978) Structure of glasses and melts of $Na_2O \cdot xSiO_2$ (x = 1, 2, 3) composition from Raman spectroscopy. Carnegie Institution of Washington Year Book, 77, 649–652.

Sweet, J. R. and White, W. B. (1969) Study of sodium silicate glasses and liquids by infrared spectroscopy. Physical Chemical Glasses, 10, 246–251.

Taylor, M., Brown, C. E., and Fenn, P. H. (1980) Structure of silicate mineral glasses. III. $NaAlSi_3O_8$ supercooled liquid at 8050°C and the effects of thermal history. Geochimica et Cosmochimica Acta, 44, 109–119.

Verweij, H. (1979a) Raman study of the structure of alkali germanosilicate glasses. I. Sodium and potassium metagermanosilicate glasses. Journal of Non-Crystalline Solids, 33, 41–53.

Verweij, H. (1979b) Raman study of the structure of alkali germano-silicate glasses. II. Lithium, sodium and potassium digermano-silicate glasses. Journal of Non-Crystalline Solids, 33, 55–69.

Virgo, D., Mysen, B. O., and Kushiro, I. (1980) Anionic constitution of silicate melts quenched at 1 atm from Raman spectroscopy; implications for the structure of igneous melts. Science, 208, 1371–1373.

Virgo, D., Seifert, F., and Mysen, B. O. (1979) Three-dimensional network structures of glasses in the systems $CaAl_2O_4$–SiO_2, $NaAlO_2$–SiO_2, $NaFeO_2$–SiO_2 and $NaGaO_2$–SiO_2 at 1 atm. Carnegie Institution of Washington Year Book, 78, 506–511.

Visser, W. and Koster van Groos, A. F. (1978) Effects of P_2O_5 and TiO_2 on the miscibility gap in K_2O–FeO–Al_2O_3–SiO_2. (abstr.) EOS, 59, 401.

Watson, E. B. (1976) Two-liquid partition coefficients: experimental data and geochemical implications. Contributions to Mineralogy and Petrology, 56, 119–134.

Watson, E. B. (1977) Partitioning of manganese between forsterite and silicate liquid. Geochimica et Cosmochimica Acta, 41, 1363–1374.

Wong, J. (1976) Vibrational spectra of vapor-deposited binary phosphosilicate glasses. Journal of Non-Crystalline Solids, 20, 83–100.

Manuscript received, November 1, 1979;
accepted for publication, August 26, 1980.